Proc. Natl. Acad. Sci. USA
Vol. 90, pp. 357–361, January 1993
Microbiology

Analysis of human immunodeficiency virus-infected tissues by amplification and *in situ* hybridization reveals latent and permissive infections at single-cell resolution

JANET EMBRETSON*, MARY ZUPANCIC*, JANET BENEKE*, MICHELE TILL†, STEVEN WOLINSKY†, JORGE L. RIBAS‡, ALLEN BURKE‡, AND ASHLEY T. HAASE*§

*Department of Microbiology, University of Minnesota Medical School, Minneapolis, MN 55455; †Department of Medicine, Northwestern University, Chicago, IL 60611; and ‡Henry M. Jackson Foundation and Department of Cardiovascular Pathology, Armed Forces Institute of Pathology, Department of Defense, Washington, DC 20306

Communicated by Dorothy M. Horstmann, October 12, 1992

ABSTRACT **Latent and productive viral infections are at the extremes of the spectrum of virus–cell interactions that are thought to play a major role in the ability of such important human pathogens as human immunodeficiency virus (HIV) to elude host defenses and cause disease. The recent development of PCR-based methods to amplify target sequences in individual cells in routinely fixed tissues affords opportunities to directly examine the subtle and covert virus–cell relationships at the latent end of the spectrum that are inaccessible to analysis by conventional *in situ* hybridization techniques. We have now used PCR *in situ* with *in situ* hybridization to document latent and permissive HIV infection in routinely fixed and paraffin-embedded tissue. In one of the first specimens we examined, a tumor biopsy from an HIV-infected individual, we found many of the lymphocytes and lymphocytes infiltrating the tumor had HIV DNA that was detectable only by PCR *in situ*. The fraction of positive cells varied regionally, but there were foci where most of the cells contained HIV DNA. Most of these lymphocytes and macrophages are latently infected, as we could detect HIV RNA in fewer than one in a thousand of these cells. We also detected HIV RNA, surprisingly, in 6% of the tumor cells, where the number of copies of viral RNA per cell was equivalent to productively infected cell lines. The alternative states of HIV-gene expression and high local concentration of latently infected lymphocytes and monocytes revealed by these studies conceptually supports models of lentiviral pathogenesis that attribute persistence to the reservoir of latently infected cells and disease to the consequences of viral-gene expression in this population. The magnitude of infection of lymphocytes documented in this report is also consistent with the emerging view that HIV infection *per se* could contribute substantially to depletion of immune cells in AIDS.**

Human immunodeficiency virus (HIV), the etiological agent of AIDS, can establish productive or latent infections in $CD4^+$ lymphocytes and monocytes in culture, and these alternative states of viral-gene expression could readily account for the devastating consequences of infection and the formidable difficulties in developing a protective vaccine (1–3). Latently infected cells could escape detection and destruction by host defenses and disseminate infection in and between individuals in the face of natural or vaccine-induced immunity. With activation of viral-gene expression, the immune system will eventually be destroyed, and the individual will succumb to a variety of opportunistic infections and unusual tumors. One critical prediction of this reconstruction of pathogenesis is that *in vivo* one can show that there is a population of infected cells that harbor the HIV provirus in a transcriptionally silent state with no detectable viral RNA and a second population in which viral transcripts are abundant. We have now used PCR-based technologies with single-cell resolution, originally developed for studies of animal lentiviruses (4–7), to provide direct experimental evidence that satisfies these predictions.

MATERIALS AND METHODS

Tissue Preparation Before PCR Amplification. Paraffin sections of tissues fixed in 4% (wt/vol) paraformaldehyde or 10% (vol/vol) buffered formalin were cut, adhered with 3% (vol/vol) Elmer's glue to glass slides coated with Denhardt's medium, heated to 60°C for 1 hr, then deparaffinized in xylene, and dehydrated in ethanol. After rehydration in phosphate-buffered saline (PBS), the sections were digested with proteinase K at 30 μg/ml in 20 mM Tris·HCl, pH 7.4/0.5% SDS for 1 hr at 37°C. After digestion, the slides were washed twice in PBS for 5 min and dehydrated in graded ethanols.

PCR Amplification. For amplification *in situ*, a solution containing PCR buffer (50 mM KCl/10 mM Tris·HCl, pH 8.3/1.5 mM $MgCl_2$/0.01% gelatin/200 μM dNTPs) and 1 μM primers was heated for 10 min to 94°C. *Taq* polymerase at 0.15 unit/μl was added after heating, and the mixture was then added to sections in volumes that ranged from 10 to 30 μl, depending on the size of the section. A multiple primer set consisting of six primers spanning nucleotides 507–2035 of the HIV (BH10) genome was used. This set generates products with overlapping cohesive termini that increase the size, and consequently the retention, of the product in fixed cells (4–7). The sections were then overlaid with a coverslip, placed in a heat-sealable plastic pouch [Kapak/Scotchpak, 4 oz (1 oz = 28.4 g), 2 mm thick] with 6–14 ml of mineral oil to prevent evaporation during thermal cycling. The bag was sealed and placed in a Bios thermal-cycler oven with a thermal sensor attached to a glass slide, similarly sealed in a bag with mineral oil. After 40 cycles of denaturation at 92°C for 2 min, annealing at 44°C for 2 min, and polymerization for 15 min at 72°C, the slides were removed from the bag and washed twice for 5 min in $CHCl_3$ to remove residual oil. After the coverslips were removed, the sections were washed once in PBS and dehydrated in graded ethanols.

The primers used for amplification were as follows: 5′-GGAACCCACTGCTTAAGCCT-3′ (bases 507–526 on the HIV HXB2cg genome), 5′-GCGTCAGTATTAAGCGGGGG-3′ (bases 801–820), 5′-GTTTTCAGCATTATCAGATG-3′ (bases 1301–1320), 5′-CATGGTGTTTAAATCTTGTG-3′ (bases 1350–1331), 5′-CCCTGGCCTTAACCGAA-

The publication costs of this article were defrayed in part by page charge payment. This article must therefore be hereby marked "*advertisement*" in accordance with 18 U.S.C. §1734 solely to indicate this fact.

Abbreviations: HIV, human immunodeficiency virus; MNC, mononuclear cell.

§To whom reprint requests should be addressed.

TTT-3′ (bases 860–841), and 5′-TTGGTGTCCTTC-CTTTCCAC-3′ (bases 2054–2035).

Detection of Amplified HIV DNA. *In situ* hybridization for HIV DNA followed published protocols (8–10). Sections were treated with 0.2 M HCl for 30 min, rinsed in water, placed in 0.153 M triethanolamine, pH 7.4, for 15 min, rinsed in water, and then rinsed in 0.05% digitonin/125 mM sucrose/3 mM Hepes, pH 7.5/0.06 M KCl for 5 min. After being rinsed in water, the sections were digested in proteinase K at 5 μg/ml in 20 mM Tris·HCl, pH 7.4/2 mM $CaCl_2$ for 15 min and then rinsed twice thoroughly for 5 min each in water before dehydrating in graded ethanols. Residual RNA was then digested with ribonucleases A and T1 (100 μg/ml and 10 units/ml, respectively) at 37°C for 30 min. Sections were washed in 2× standard saline citrate (SSC)/0.1% diethyl pyrocarbonate for 5 min and then in 2× SSC for an additional 5 min. Cells were then postfixed in 4% (wt/vol) paraformaldehyde for 2 hr. Before denaturation, cells were washed twice in 2× SSC and acetylated in 0.25% acetic anhydride/0.1 M triethanolamine, pH 8.0, for 10 min. Denaturation was in 95% (vol/vol) formamide/0.1× SSC for 15 min at 68°C. Cells were chilled briefly in 0.1× SSC at 4°C and then dehydrated in graded ethanols.

Sections were hybridized to either a radiolabeled full-length HIV or heterologous Visna virus probe derived from digestion of cloned DNA and purification of viral sequences after separation by agarose gel electrophoresis. Probes were labeled by nick translation to specific activities of $\approx 10^9$ dpm/μg with ^{125}I-labeled dCTP or ^{35}S-labeled dATP and ^{35}S-labeled dCTP. After hybridization and washes in 2× SSC and formamide, sections were dehydrated in graded ethanols containing 0.3 M ammonium acetate, coated with NTB2 nuclear track emulsion (Kodak), exposed at 4°C, developed, and counterstained with hematoxylin/eosin or Wright–Giemsa stain.

Detection of HIV RNA by *in Situ* Hybridization. Detection of HIV RNA also followed published procedures (8–10). After pretreatments to enhance diffusion, the sections were hybridized to the full-length BH10 HIV or Visna virus probe, washed, coated with emulsion, developed, and stained.

Immunocytochemistry. Eight-micrometer sections were deparaffinized in xylene and treated with methanol for 10 min and then treated with 0.5% H_2O_2/methanol for 20 min to block endogenous peroxidase activity. After the slides were washed twice for 2 min in PBS, the sections were digested at 37°C for 7 min with Pronase E at 67 μg/ml in PBS. After six washes in PBS (5 min each), nonspecific binding of antibody was blocked with horse serum in PBS, according to the manufacturer's (Vector Laboratories) protocols. The tissues were then incubated at room temperature for 60 min with primary monoclonal antibodies diluted in PBS to cytokeratins [1:75 dilution of antibody MAK-6 from Triton Biosciences (Alameda, CA) and 1:400 dilution of antibodies AE-1 and AE-3 from Hybritech], to CD4 (OPD4 from DAKO diluted 1:75; CD3 from DAKO diluted 1:100), or macrophages [KPI-CD68 from DAKO (Carpinteria, CA) diluted 1:200]. After being washed briefly in PBS, the sections were incubated at room temperature for 60 min with biotinylated secondary antibody (anti-goat IgG in PBS/5% nonfat milk), washed again with PBS, and then treated with avidin–biotin horseradish peroxidase complex (Vectastain Elite ABC Kit, Vector Laboratories). After being washed in PBS, the sections were placed in PBS with diaminobenzidine at 140 μg/ml and 0.1% H_2O_2, washed in PBS, and counterstained with hematoxylin. For negative controls, normal mouse ascites (ICN) or sera were substituted for the primary antibody in a subjacent tissue section.

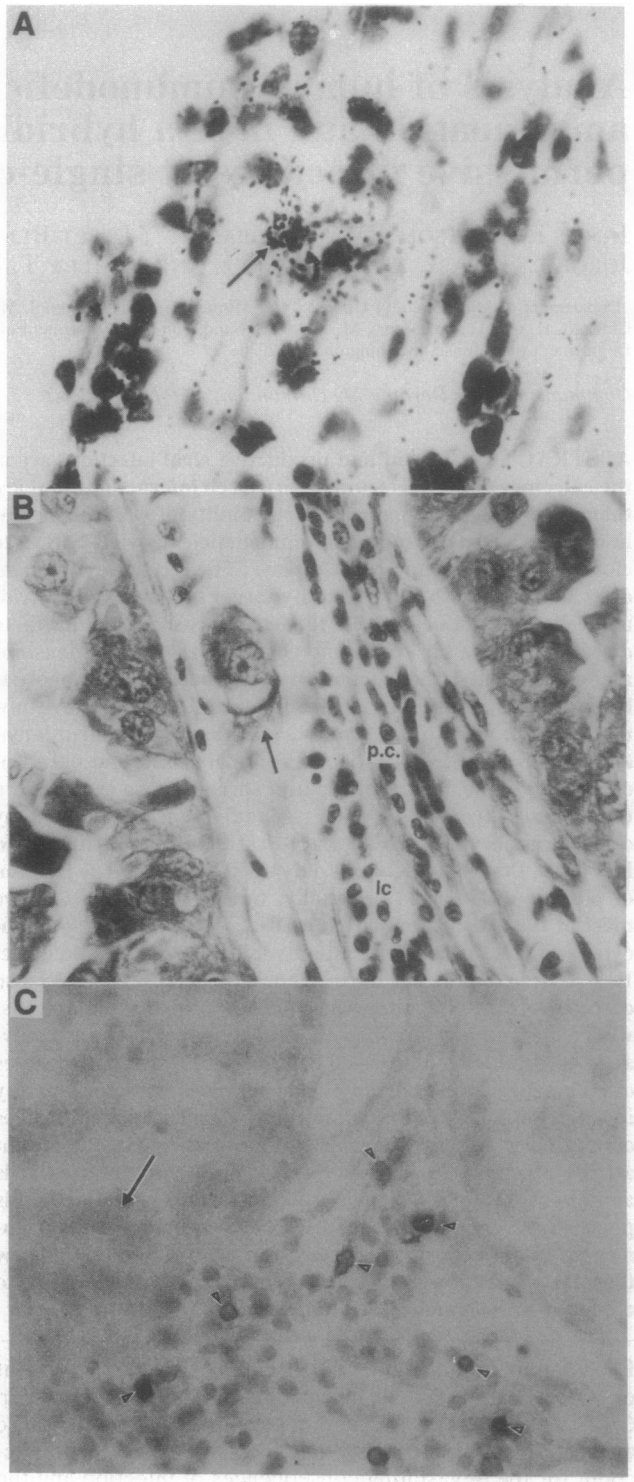

FIG. 1. (*A*) Detection of HIV RNA lymphocytes and monocytes in a tissue biopsy and characterization of the cells. Sections from the biopsy were hybridized to an HIV-specific probe as described in refs. 11–13. The arrow indicates a cell with HIV RNA in collections of MNCs infiltrating a tumor. (*B* and *C*) Sections of the biopsy were treated sequentially with monoclonal antibodies to cytokeratin (*B*) or CD4 (*C*), biotinylated antibody to IgG of the primary antibody, avidin–biotin horseradish peroxidase complex, and diaminobenzidine and H_2O_2. The sections were subsequently counterstained with hematoxylin. In *B* (×400), there are brown-staining cytokeratin-positive adenocarcinoma cells with vacuoles (arrow) and unstained MNCs that include plasma cells (p.c.), other lymphocytes (lc), and monocytes/macrophages. Some of the MNCs are $CD4^+$ (arrowheads) (*C*), whereas the adenocarcinoma cells (arrow) are $CD4^-$.

RESULTS AND DISCUSSION

To directly investigate HIV-gene expression in tissues, we initially surveyed a limited collection of specimens on hand to identify one in which we could detect HIV RNA and found HIV RNA in lymphocytes (Fig. 1*A*) and macrophages in a biopsy from an HIV-infected individual with moderate decrease in the T4 subset ($CD4^+$ lymphocyte count blood of 260 per μl). We subsequently focused our analysis of HIV–host-cell interactions on this specimen, which turned out to be a tumor heavily infiltrated by monocytes, macrophages, plasma cells, and lymphocytes (Fig. 1*B*), of which 23% were $CD4^+$ (Fig. 1*C*, Table 1). The tumor was a papillary adenocarcinoma in the brain that had metastasized from a primary tumor in the lung.

We could not detect HIV DNA by conventional *in situ* hybridization in either the mononuclear cells (MNCs) or tumor cells (Fig. 2*A*) in this tissue, but after amplification *in situ* we found HIV DNA in the nuclei of MNCs that by morphological criteria we classified as lymphocytes and monocytes, in a ratio of ≈2:1. The proportion of infected MNCs varied throughout and between tissue sections, from individual cells in infiltrates (Fig. 2*B*) to follicle-like collections in which most of the cells contained HIV DNA (Fig. 2*C*). Surprisingly, we also detected HIV DNA in the tumor cells (Fig. 2 *D* and *E*) but did not detect HIV DNA in plasma cells, polymorphonuclear leukocytes, endothelial cells, or erythrocytes. HIV DNA was well localized to the nuclei of MNCs and tumor cells (Fig. 2), and there was no hybridization signal in adjacent cells. This is in accord with our initial observations (4–7) in a lentivirus animal model and with more recent experience of other investigators with HIV (11–13, 16) that amplified DNA products are retained in cells under appropriate conditions and do not leak into adjacent cells to generate spurious false positive signals in uninfected cells. The amplification and detection of HIV DNA in the MNCs and tumor cells are specific, as (*i*) there was no hybridization to a heterologous probe (Visna virus) in identically treated adjacent sections (Fig. 2*F*); and (*ii*) the HIV probe bound at background levels to lymphocytes and monocytes in lymph node and tonsillar tissue from HIV-seronegative individuals or carcinoma cells from HIV-seronegative individuals (Table 1). The observations were also reproducible in six independent experiments.

To determine the proportion of MNCs with HIV DNA, we compared the frequency distribution of grains per MNC in the infected tissue sections with MNCs in tissues from uninfected controls that had been fixed and processed in the same way (Table 1). Fig. 3 shows one such comparison of the frequency distribution of grain counts in a control and one area of the tissue section of the infected individual, where 34% of the MNCs are in a nonoverlapping distribution with 10–30 grains per cell. Although amplification in fixed tissues is inefficient (compared with DNA in solution), the mean grain count per cell is 10 times that of the control, and infected cells are easily and reliably distinguished from uninfected MNCs. In 10 other randomly chosen fields with ≈1000 cells, we detected HIV DNA in 15% of the MNCs; the range was from <1% to 27%. The tumor cells with HIV DNA were more uniformly distributed, and amplification was also 5-fold or more higher than in MNCs for reasons that we do not as yet understand. This increase in signal simplified the estimate of tumor cells containing HIV DNA (6%), as the positive cells were readily identified as those with grains too numerous to count (compare Fig. 2 *D* and *E*) against a negligible background in the uninfected cells. The HIV-infected individual from whom the biopsy had been taken was lost to follow-up, and we were, thus, unable to obtain additional tumor or other tissues or blood. We, therefore, could not evaluate the likelihood that (*i*) infected tumor cells disseminated HIV to invading lymphocytes or monocytes or that (*ii*) invading lymphocytes or monocytes transmitted infection to tumor cells, and ensuing viral replication contributed to the extensive infection in both populations.

Thermal cycling denatures antigens, and we have not yet been able to devise conditions to unequivocally determine by double-label techniques of immunocytochemistry and *in situ* hybridization (17) whether or not the lymphocytes containing

Table 1. Characteristics of HIV–cell interactions *in vivo*

Cell type	HIV DNA,* %	HIV RNA,† %	Estimated RNA copy number†	Inflammatory cell infiltrates,‡ %			
				T lymphocytes	$CD4^+$ lymphocytes	Monocytes/ macrophages	B (plasma) cells
MNCs in inflammatory infiltrates	15.3	<0.1		69	23	11	20
Adenocarcinoma	5.9	5.9	250–500				

*After amplification and *in situ* hybridization, tissue sections from the tumor of the HIV-seropositive individual or from lymph node, tonsil, or squamous cell carcinoma from seronegative individuals were coated with NTB2, exposed for 3–4 days, developed, and stained. The efficiency of amplification *in situ* was greater in the adenocarcinoma cells compared with the lymphocytes and monocyte/macrophages, so that the fraction of cells with HIV DNA could be determined by simply scoring as positive those cells with grains too numerous to count in 10 randomly selected fields with ≈1000 cells. For the MNCs, background binding of the HIV probe to lymphocytes in tissue sections of lymphoid organs from the seronegative controls was determined by counting silver grains over 100 randomly selected cells. With a 4-day exposure, these counts averaged 1.3 and 1.6 grains per cell on duplicate determinations with a range of 0–9 grains per cell. One hundred MNCs in an inflammatory infiltrate near the focus shown in Fig. 2*C* from the HIV-seropositive individual were examined, and those with ≥10 grains per cell with no overlap with the control distribution were scored as positive (see Fig. 3). In 10 randomly selected fields with ≈1000 cells, 15% of the lymphocytes and monocytes were scored as positive by the same criterion; the range was <1% to 27%. Data from Fig. 3 and a rare focus with >90% positives shown in Fig. 2*C* were not included in the fields used to determine the mean.

†After *in situ* hybridization for RNA, tissue sections from the seropositive individual and seronegative controls were coated with NTB2 and exposed for 6–10 days. There was no difference in average grain count per cell (5.0) and range in the controls and ≈1000 MNCs in the inflammatory infiltrates, but 59/1000 adenocarcinoma cells had grains over the nucleus and cytoplasm too numerous to count and were scored as positive. The relative abundance of HIV RNA in the adenocarcinoma cells vis-à-vis productive infections in lymphoblastoid (H9) cells was determined by comparing grain counts in the tumor (*i*) with sections of HIV-infected H9 cells concentrated by centrifugation, fixed in formalin, and embedded in paraffin or (*ii*) with formalin-fixed and paraffin-embedded productively infected lymphoma cells maintained as a s.c. tumor in irradiated nude mice. With a radioautographic exposure of 1 day, the adenocarcinoma cells with HIV RNA had an average grain count of 29.2 per cell; the range was 17–49; the lymphoma cell average was 29.6; the range was 16–62. Because productively infected lymphoma cells have been estimated to contain 250–500 copies of viral RNA per cell, there are approximately the same number of transcripts per cell in the epithelial tumor cells (14, 15).

‡Tissue sections of tumor from the seropositive individual were treated with antibodies that identify T lymphocytes (anti-CD3), the $CD4^+$ subset (OPD4), and monocytes/macrophages (KPI-CD68). After immunocytochemical development, stained cells in 500 cells in inflammatory infiltrates were enumerated. Plasma cells in the infiltrates were identified by morphological criteria. The CD8 population was estimated by difference to be 47%.

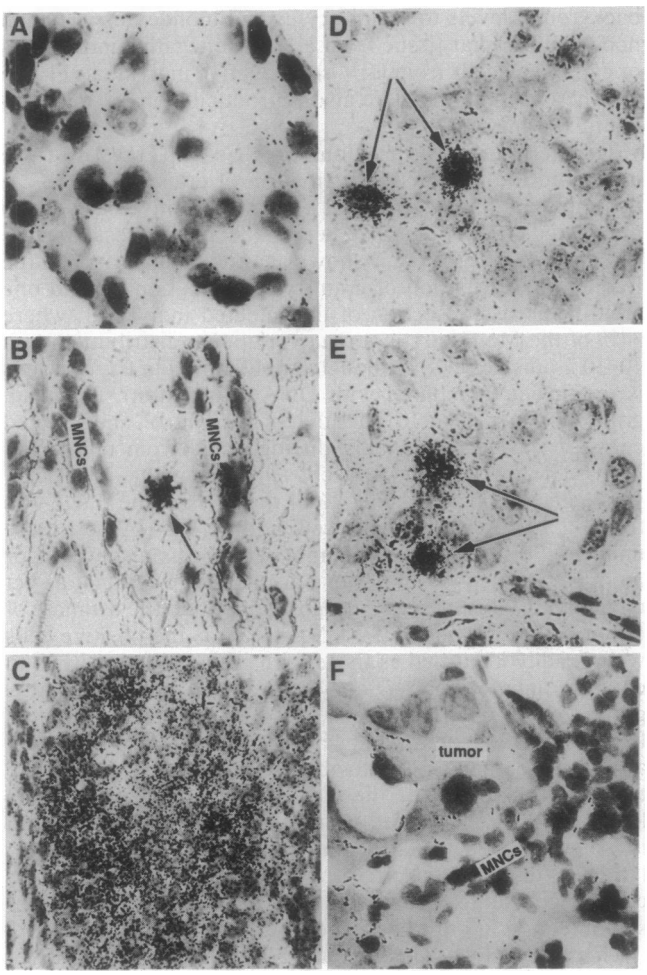

FIG. 2. Detection of HIV DNA in individual cells in tissue sections by PCR *in situ*. Tissue sections were pretreated and hybridized to an HIV-specific probe by using conventional methods (*A*) or after amplifying target sequences *in situ* by PCR (*B–F*), as described. In the developed stained radioautographs, the number of silver grains over the cells (*A*) was indistinguishable from lymphocytes or carcinoma cells in, respectively, lymph node, tonsil, or tumor specimens from HIV-seronegative individuals (data not shown). However, after amplification, HIV DNA could be easily detected in lymphocytes, either single cells (*B*, arrow) in MNC collections around small blood vessels or in follicular collections of HIV-positive lymphocytes (*C*), and in adenocarcinoma cells of the HIV-infected individual (*D* and *E*, arrows). Level of HIV DNA after amplification of background binding to a heterologous probe (Visna virus DNA radiolabeled with ^{35}S to a specific activity equivalent to the HIV probe (*F*). (×260.) Radioautographic exposure time was 6 days (*A*) or 3 days (*B–F*).

HIV DNA were exclusively in the $CD4^+$ helper subset. However, this grouping is clearly the most probable. Judging from their staining with antibodies to cytokeratins (Fig. 1*B*) but not to CD4 (Fig. 1*C*), the tumor cells are of epithelial origin and $CD4^-$. Although this result is consistent with other lines of evidence that HIV can enter cultured neural and colonic epithelial cells by an alternative receptor or other mechanisms (18–21), it is also possible that the tumor cells do not have CD4 on their surface in sufficient quantity or lack the epitope required for recognition by the monoclonal antibody used for typing. We favor the latter interpretation, as we detect CD4 mRNA in *in situ* hybridization in the tumor cells as well as lymphocytes in the infiltrates (data not shown).

For the most part, lymphocytes and macrophages in this tissue harbor HIV in a latent state, as we could detect viral

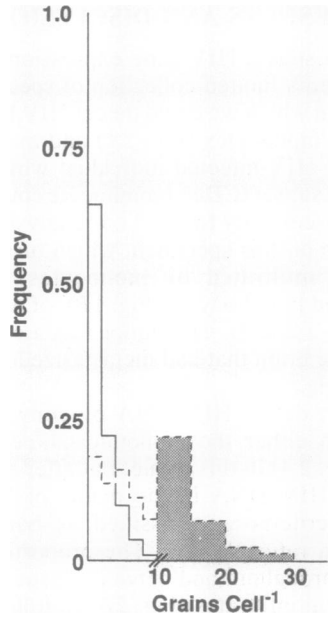

FIG. 3. Frequency distribution of grain counts over lymphocytes and monocytes/macrophages after amplification of HIV DNA and *in situ* hybridization. Silver grains over the nuclei of MNCs in an inflammatory infiltrate in the tumor tissue of an HIV-seropositive individual (- - -) or lymphoid tissue from uninfected controls (——) were enumerated, as described in Table 1. The region of the frequency distribution where there is no overlap between the control and infected distributions (≥10 grains per cell) is shaded to highlight the population scored as positive for HIV DNA.

transcripts by *in situ* hybridization only rarely (less than one in a thousand cells), a frequency similar to that observed by Harper *et al.* (14) in lymph node and peripheral blood. By contrast, we detected viral RNA in the nucleus and cytoplasm in the same proportion of tumor cells that contained HIV DNA, and the abundancy of transcripts was equivalent to that detected in lymphoblastoid cells productively infected with HIV (14) and grown as a tumor in nude mice (15) (Fig. 4, Table 1).

By combining PCR *in situ* with quantitative *in situ* hybridization, we thus have shown *in vivo* that there is a spectrum of virus–host relationships that encompasses and conceptually unifies the mechanisms by which HIV and animal lentiviruses persist and cause disease (1–3, 22). Latent infections provide a reservoir to perpetuate and disseminate infection despite host defenses. Our studies suggest that the reservoir will be composed both of $CD4^+$ lymphocytes, in agreement with a similar conclusion based on PCR analyses of populations of cells sorted from peripheral blood (23), but also cells in the monocyte lineage. Our much higher estimate of the extent of infection of MNCs is consistent with recent reevaluations of the percentage of peripheral blood MNCs with HIV DNA by "booster" as well as *in situ* PCR techniques (11–13, 16, 24) and points to the possibility that quite a large reservoir exists at later stages of infection. Even these estimates may be low, if the high local concentrations of covertly infected cells we observed in this tissue specimen (>30% of lymphocytes in focal areas) is mirrored in lymph node and other lymphoid organs currently thought to be a major component of the reservoir (25–31).

At the other end of the spectrum are the MNCs, and, in this specimen, tumor cells, in which there is evidence of viral-gene expression. Activation of viral-gene expression in lymphocytes could play a larger and direct role in depletion of immune cells, given the large population of infected, presumably $CD4^+$, lymphocytes. These cells and others in this specimen probably have only a single copy of HIV DNA that

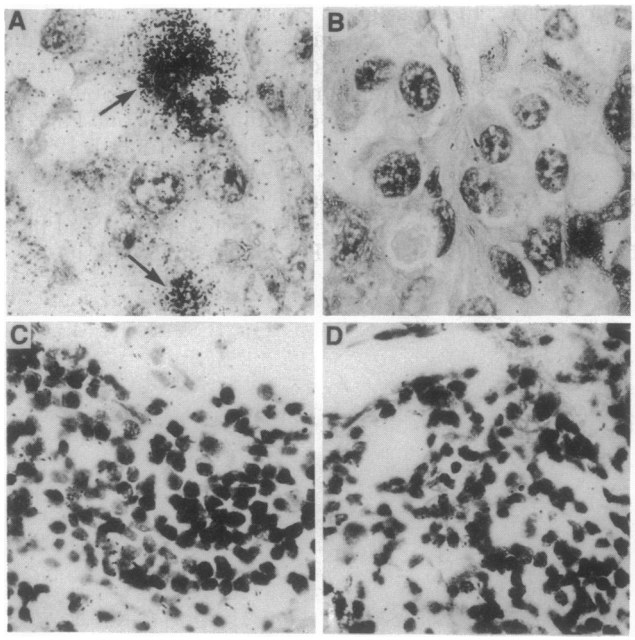

FIG. 4. Detection of HIV RNA by *in situ* hybridization. Tissue sections were hybridized to HIV-specific probe to detect viral RNA as described (11–13). Viral transcripts are abundant in the adenocarcinoma cells (*A*, arrow) but are undetectable in most MNCs in the inflammatory cell infiltrates (*C*). Background levels of binding of heterologous Visna virus probe to adenocarcinoma (*B*) and MNCs (*C* and *D*) are illustrated. Radioautographic exposures were 6 days. (×225.)

would not be identified as infected cells by *in situ* hybridization, which has practical limits in sensitivity of detection of two retroviral genomes per cell (11–13). It should now be possible with the advances in single-cell technologies to quantitatively assess the progression of infection in the course of HIV infection and the relationship of the extent of infection to immune depletion, monitor response to treatment, and, more generally, gain new insights into how many and what kinds of cells viruses infect.

We thank Colleen O'Neill and Tim Leonard for preparation of the manuscript, Drs. Robert Levy and Neal Wetherall for providing tissue samples and HIV-infected lymphoblastoid tumors from nude mice, and the National Institutes of Health for support.

1. Fauci, A. S. (1988) *Science* **239,** 617–622.
2. Levy, J. A. (1988) *Nature (London)* **333,** 519–522.
3. Greene, W. C. (1991) *N. Engl. J. Med.* **324,** 308–317.
4. Staskus, K. A., Couch, L., Bitterman, P., Retzel, E. F., Zupancic, M., List, J. F. & Haase, A. T. (1991) *Microb. Pathol.* **11,** 67–76.
5. Haase, A. T., Retzel, E. F. & Staskus, K. A. (1990) *Proc. Natl. Acad. Sci. USA* **87,** 4971–4975.
6. Retzel, E. F., Staskus, K. A., Embretson, J. E. & Haase, A. T. (1992) in *PCR Protocols* (Academic, New York), in press.
7. Embretson, J. E., Staskus, K. A., Retzel, E. F., Haase, A. T. & Bitterman, P. (1992) in *The Polymerase Chain Reaction* (Immune Response Corp., San Diego), in press.
8. Haase, A. T., Stowring, L., Harris, J. D., Traynor, B., Ventura, P., Peluso, R. & Brahic, M. (1982) *Virology* **119,** 399–410.
9. Haase, A. T., Brahic, M., Stowring, L. & Blum, H. (1984) *Methods Virol.* **7,** 189–226.
10. Haase, A. T. (1987) in *In Situ Hybridization: Applications to Neurobiology*, eds. Valentino, K. L., Eberwine, J. H. & Barchas, J. D. (Oxford Univ. Press, New York), pp. 197–219.
11. Nuovo, G. J., MacConnell, P., Forde, A. & Delvenne, P. (1991) *Am. J. Pathol.* **139,** 847–854.
12. Nuovo, G. J., Gallery, F., MacConnell, P., Becker, J. & Bloch, W. (1991) *Am. J. Pathol.* **139,** 1239–1244.
13. Nuovo, G. J., Margiotta, M., MacConnell, P. & Becker, J. (1992) *Diagn. Mol. Pathol.* **1,** 98–102.
14. Harper, M. E., Marselle, L. M., Gallo, R. C. & Wong-Staal, F. (1986) *Proc. Natl. Acad. Sci. USA* **83,** 772–776.
15. Weatherall, N. T. (1990) in *Animal Models in AIDS*, eds. Schellekens, H. & Horzinek, M. C. (Elsevier, Amsterdam), pp. 291–302.
16. Bagasra, O., Hauptman, S. P., Lischner, H. W., Sachs, M. & Pomerantz, R. J. (1992) *N. Engl. J. Med.* **326,** 1385–1391.
17. Brahic, M. & Haase, A. T. (1989) *Curr. Top. Microbiol. Immunol.* **143,** 9–20.
18. Bhat, S., Spitalnik, S. L., Gonzalez-Scarano, F. & Silberberg, D. H. (1991) *Proc. Natl. Acad. Sci. USA* **88,** 7131–7134.
19. Fantini, J., Yahi, N. & Chermann, J.-C. (1991) *Proc. Natl. Acad. Sci. USA* **88,** 9297–9301.
20. Fantini, J., Yahi, N., Baghdiguian, S. & Chermann, J.-C. (1992) *J. Virol.* **66,** 580–585.
21. Phillips, D. M. & Bourinbaiar, A. S. (1992) *Virology* **186,** 261–273.
22. Haase, A. T. (1986) *Nature (London)* **322,** 130–136.
23. Schnittman, S. M., Psallidopoulos, M. C., Lane, H. C., Thompson, L., Baseler, M., Massari, F., Fox, C. H., Salzman, N. P. & Fauci, A. S. (1989) *Science* **245,** 305–308.
24. Hsia, K. & Spector, S. A. (1991) *J. Infect. Dis.* **164,** 470–475.
25. Parmentier, H. K., van Wichen, D., Sie-Go, D. M., Goudsmit, J., Borleffs, J. C. & Schuurman, H. J. (1990) *Am. J. Pathol.* **137,** 247–251.
26. Armstrong, J. A. & Horne, R. (1984) *Lancet* **ii,** 370–372.
27. Baroni, C. D., Pezzella, F., Mirolo, M., Ruco, L. P. & Rossi, G. B. (1986) *Histopathology* **10,** 5–13.
28. Spiegel, H., Herbst, H., Niedobitek, G., Foss, H.-D. & Stein, H. (1992) *Am. J. Pathol.* **140,** 15–22.
29. Pantaleo, G., Graziosi, C., Butini, L., Pizzo, P. A., Schnittman, S. M., Kotler, D. P. & Fauci, A. S. (1991) *Proc. Natl. Acad. Sci. USA* **88,** 9838–9842.
30. Fox, C. H., Tenner-Rácz, K., Rácz, P., Firpo, A., Pizzo, P. A. & Fauci, A. S. (1991) *J. Infect. Dis.* **164,** 1051–1057.
31. Rácz, P., Tenner-Rácz, K., Kahl, C., Feller, A. C., Kern, P. & Dietrich, M. (1986) *Prog. Allergy* **37,** 81–181.